Ceramics-Silikáty 64 (1), 40-49 (2020)
www.ceramics-silikaty.cz doi: 10.13168/cs.2019.0047

SILICA-BASED CERAMIC MATERIALS FOR INVESTMENT CASTING: THE EFFECT OF ALUMINA NANOPARTICLES

XIAO CHEN*, CHUNYANG LIU**, WENLONG ZHENG**, JIQING HAN**, LI ZHANG**, CHUNMING LIU*

*School of Materials Science and Engineering, Northeastern University, Shenyang 110819, Liaoning, the People's Republic of China
**School of Metallurgy, Northeastern University, Shenyang 110819, Liaoning, the People's Republic of China

#E-mail: fantai320@163.com

Submitted July 23, 2019; accepted September 16, 2019

Keywords: Alumina nanoparticles, Silica-based ceramic core, Cristobalite crystallisation, Flexural strength, Open porosities

Silica-based ceramic cores containing various contents of alumina nanoparticles were prepared by ceramic injection moulding with zircon as a sintering aid. The alumina nanoparticles were introduced into the mixture in the form of a colloidal sol. The phase evolution and morphology of the sintered ceramic specimens were analysed by X-ray diffraction (XRD) and scanning electron microscopy equipped with energy dispersive spectrometry (SEM/EDS), respectively. Three-point bending tests were carried out on all of the prepared ceramic specimens. The results showed that the addition of alumina nanoparticles not only promoted the crystallisation of the fused silica, but also increased the formation of a liquid phase in the silica-based ceramic specimens during the sintering. The increased formation of a liquid phase was mainly attributed to the presence of Al, Na and K elements in the alumina nanoparticles, which diffused as a liquid phase into the pores between the silica particles and improved the densification. The flexural strength of the sintered ceramic specimens was improved by adding a proper amount of alumina nanoparticles, which could be attributed to the reinforcement of the sintering necks between the particles and the strengthening of the silica particles

INTRODUCTION

Ceramic cores are extensively utilised as high temperature structural materials, especially in investment metal casting, which are used to form intricate internal cooling passages in superalloy gas turbine blades [1-3]. In the process of investment metal casting, ceramic cores need to withstand a thermal stress at elevated temperatures [4]. Therefore, ceramic cores are manufactured using a mixture of refractory material particles.

Fused silica is widely used as a core material due to its low thermal expansion coefficient ($0.55 \times 10^{-6}\cdot K^{-1}$ between 25 and 1000 °C), excellent chemical inertness against molten metal and easy removal by a harmless process for the cast [5-8]. However, it has been reported that the flexural strength of the fused silica as the core material does not exceed 6 MPa [9]. Therefore, a number of researchers have developed methods to improve the flexural strength of sthe ilica-based ceramic cores, especially in microscale ceramic additives [10-13]. Kim et al. [14] investigated the effect of SiC on the flexural strength of silica-based ceramic cores. The results showed that SiC accelerated the formation of cristobalite in the silica-based composites. The increase in the SiC content resulted in an increase in the flexural strength, since the strength of cristobalite is higher than that of the fused silica. Kazemi et al. [15] suggested that the addition of zircon could increase the flexural strength of the silica-based ceramic cores. This is because the strength of the zircon particles is higher than that of the fused silica particles.

Many researchers have focused on adding microscale additives to the matrix, but it has been shown that nanoscale additives may improve the flexural strength more than the microscale additives [16]. Even low volume fractions of nanoparticles have a significant effect on the mechanical properties of nanocomposites [17, 18]. Liu et al. [19] introduced tungsten carbide (WC) nanoparticles into silicon nitride ceramics. Compared to the specimens without the WC nanoparticles, the flexural strength of the specimens containing the WC nanoparticles increased markedly. They thought that the uniform dispersion of the WC nanoparticles in the ceramic matrix produced a dispersion-strengthening mechanism, which increased the flexural strength of the Si_3N_4 ceramics. Therefore, to investigate the influence of nanoscale additives on the flexural strength of silica-based ceramic cores, the cristobalite crystallisation behaviour and the mechanical properties of the silica-based ceramic specimens with different alumina nanoparticle additions (0.5; 1.0; 1.5; 2.0 and 2.5 wt. %) are investigated in the present study.

EXPERIMENTAL

Fabrication of the silica-based ceramic cores

Figure 1 shows the feedstock preparation procedure and the heat treatment for the ceramic cores. The mixture used for the fabrication of the silica-based ceramic cores consisted of fused silica (Amorphous SiO_2, 98.76 %, Lianyungang Hongding Quartz Co., Ltd., China) with various particle sizes ranging from 15 to 50 μm, zircon ($ZrSiO_4$, 10 μm, 94.49 %, Weifang Huazhong New Composite Material Co., Ltd., China) and alumina nanoparticles. To disperse the nanoparticles homogenously, the alumina nanoparticles were added to the mixture in the form of a colloidal sol (alumina oxide, 10 - 20 nm, 40 % in H_2O, colloidal dispersion). The fused silica powders, zircon powders and alumina colloidal sol were ball milled at room temperature for 6 h, using deionised water as a medium and agate as the mixing balls. The resulting mixture was dried and sieved to obtain ~200 mesh particles. Finally, the feedstock was prepared by mixing the obtained particles with a thermoplastic (paraffin wax, microcrystalline and polyethylene) at 80 °C under vacuum.

Silica-based ceramic specimens with different concentrations of alumina nanoparticles (0; 0.5; 1.0; 1.5; 2.0 and 2.5 wt. %), denoted as FNA-0, FNA-0.5, FNA-1, FNA-1.5, FNA-2 and FNA-2.5, respectively, were fabricated using ceramic injection moulding. An increase in the alumina nanoparticle content was accompanied by a decrease in the fused silica content, while the zircon content was always 10 wt. %. First, the fabricated ceramic bar specimens (120 × 10 × 4 mm^3) were heated to 450 °C at 1.33 °C·min^{-1} and held at this temperature for 2 h to remove the organic binders. To provide good support and prevent the deformation or cracks in the specimens during the binder removal process, an industrial alumina powder with a purity of 99.6 % and average particle size of approximately 91.9 μm was used as a powder bed. After burning out the organic binders by the low temperature heating, the specimens were sintered at a heating rate of 2 °C·min^{-1} up to 900 °C for 0.5 h to improve the temperature uniformity of the ceramics. Then, the specimens were heated at 1250 °C and 1300 °C for 2 h to form entire porous ceramics.

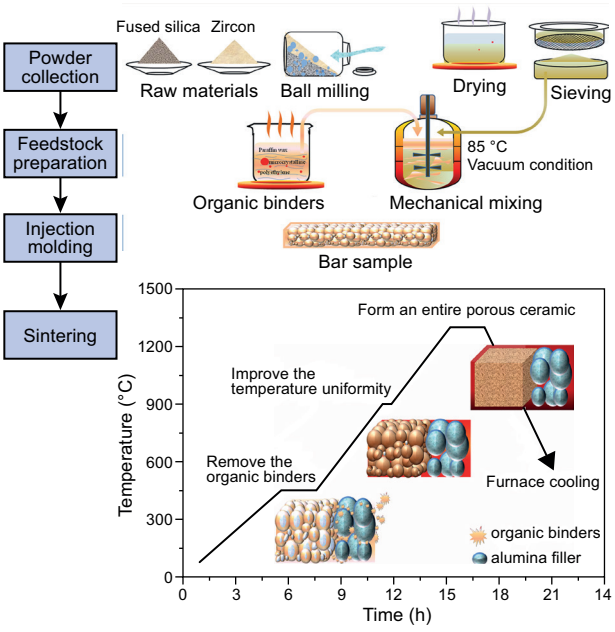

Figure 1. The schematic of the ceramic core feedstock preparation and heat treatment.

Characterisation

The phase and morphology of the sintered silica-based ceramic cores with different concentrations of alumina nanoparticles were identified by X-ray powder diffraction (XRD, Smart Lab 9 kW, Rigaku, Japan) using Ni-filtered Cu Kα radiation and scanning electron microscopy (SEM/EDS, Quanta250FEG, FEI, America), respectively. To study the influence of the alumina nanoparticles on the crystallisation of cristobalite in the silica-based ceramic cores, the cristobalite and zircon peak heights were extracted from the original XRD data by the software Jade 6. The quantification of the cristobalite in the ceramic cores could be conducted using the reference intensity ratio (RIR) method [20].

To investigate the influence of the alumina nanoparticles on the flexural strength of the silica-based ceramic cores, the sintered specimens were subjected to a three-point bending test using a 5 N·s^{-1} loading rate and a span distance of 30 mm on a universal testing machine (UTM, AG-XPlus, Shimadzu, Japan) according to HB 5353.3 2004. The open porosities of all of the specimens were also measured by the Archimedes method, HB 5353.1 2004, using distilled water as the immersion fluid. Each reported result was the average of three tests.

RESULTS AND DISCUSSION

Characterisation of the silica-based ceramic cores

The XRD patterns of the silica-based ceramic cores with different concentrations of alumina nanoparticles and sintered at different temperatures are shown in Figure 2. Figure 3 shows the changes of the main peak ratio of the cristobalite and zircon in the sintered ceramic cores. The characteristic diffraction peaks for the cristobalite phase can be seen in all of the specimens, regardless of the alumina nanoparticle content. This demonstrates that the cristobalite is always formed by crystallisation of the fused silica during the sintering. The amount of alumina nanoparticles in the specimens is so small that it cannot be detected by XRD, but analysis of the EDS data can indicate the existence of the alumina nanoparticles. Compared to the EDS

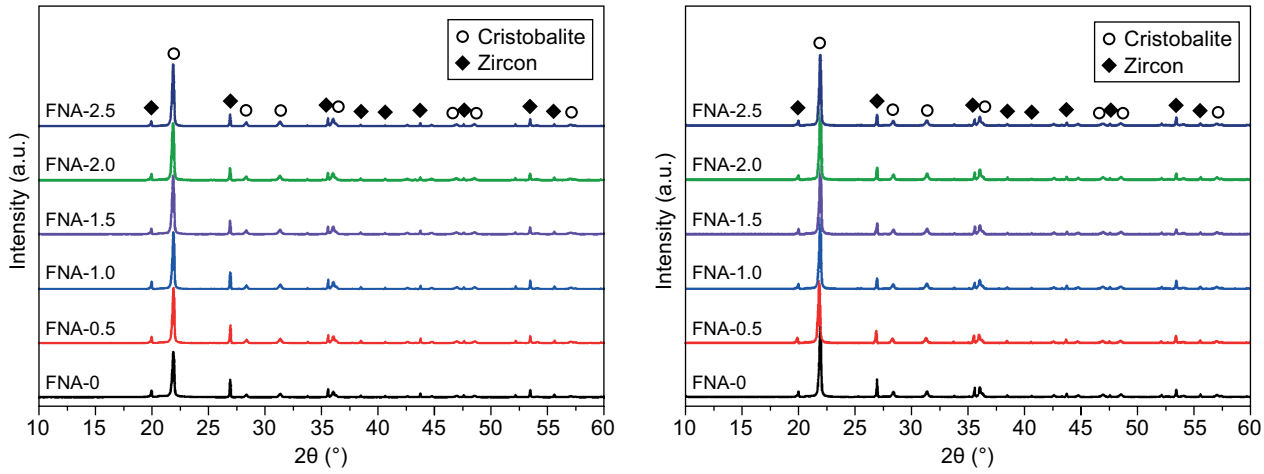

Figure 2. The XRD patterns of the silica-based ceramic specimens with the different alumina nanoparticle concentrations and sintered at the different temperatures: a) 1250 °C; b) 1300 °C.

data for specimen FNA-0, which does not contain any alumina nanoparticles, the alumina peaks are clearly observed in specimen FNA-2, as shown in Figure 4b.

The cristobalite contents, calculated using the reference intensity ratio (RIR) method, were 22.1 % for FNA-0, 27.4 % for FNA-0.5, 35.9 % for FNA-1, 39.9 % for FNA-1.5, 42.4 % for FNA-2 and 45.9 % for FNA-2.5 when the specimens were sintered at 1250 °C. In contrast, they were 32.7 % for FNA-0, 46.5 % for FNA-0.5, 52.8 % for FNA-1, 58.3 % for FNA-1.5, 60.2 % for FNA-2 and 61.3 % for FNA-2.5 when the specimens were sintered at 1300 °C, which are significantly higher than those of the specimens that were sintered at 1250 °C. With the increase in the sintering temperature, the crystallisation of the specimens fabricated with the same powders increases. This result is consistent with that of Kazemi et al. [21]. In addition, the use of alumina nanoparticles increases the formation of cristobalite regardless of the sintering temperature. Liang et al. [10] demonstrated that the addition of alumina microparticles promoted the crystallisation of the fused silica during the sintering. When the alumina microparticle concentration increased from 5 wt. % to 10 wt. %, the amount of cristobalite increased from 25 % to 40 % at 1220 °C. They believed that when the molar ratio of the alkali and alkaline oxide to the alumina was less than a unit, the dissolved alumina acted as a modifier, increasing the number of the non-bridged oxygen atoms and the diffusion mobility of the SiO_4 tetrahedrons and, consequently, leading to a higher tendency towards the crystallisation of the amorphous silica particles. Compared to the addition of alumina microparticles, the addition of the alumina nanoparticles enhances the tendency toward the crystallisation of the fused silica. This is related to the amount of the dissolved alumina in the fused silica grains. As shown in Figure 5a, a large number of the fused silica particles aggregate around the alumina microparticle. The EDS point analysis results for fused silica particle A are summarised in Table 1, revealing that the aluminium content decreases as the distance from alumina particle B increases. This result suggests that the alumina enables the diffusion and can be dissolved in the amorphous fused silica particles.

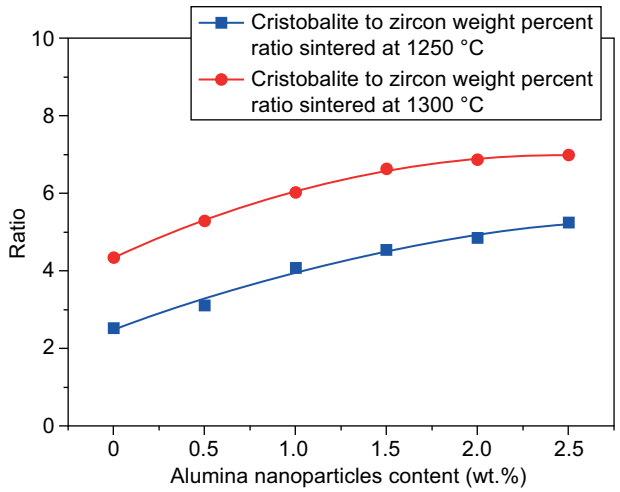

Figure 3. The cristobalite to zircon main peak ratio in the sintered ceramic specimens.

Table 1. The results of the EDS point analyses in fused silica particle A.

Composition (wt. %)	1	2	3	4	5
Al	0.28	0.52	1.08	4.11	18.66
Si	38.03	35.72	33.01	31.68	21.45
O	61.68	63.76	65.92	64.21	59.89

Alumina nanoparticles are distributed on the fused silica particles' surfaces. The smaller particle size and larger specific surface area increases the alumina diffusion rate, and, consequently, increases the amount of the alumina dissolved in the fused silica grains. As shown in Figure 5b, when the same concentration of alumina nanoparticles is added, the aluminium is evenly distributed on the silica grain surface in the specimen after sintering at 1300 °C.

The structural characterisation of specimens FNA-0 and NFA-2 that were sintered at 1250 °C was conducted using SEM, as shown in Figure 6. Specimen FNA-2 has a bigger liquid phase than FNA-0. Figure 6c shows that, the particles are bonded to each other by

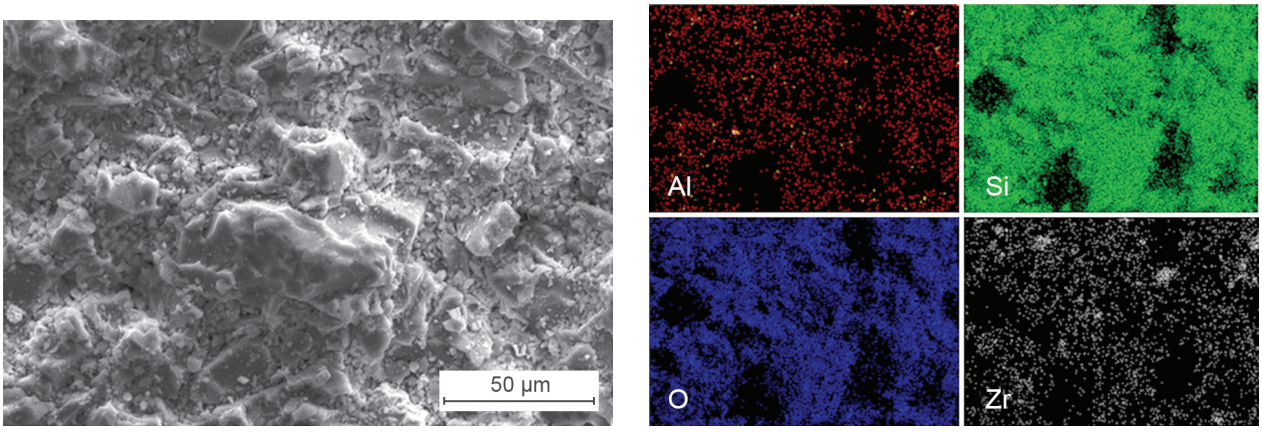

a) FNA-0

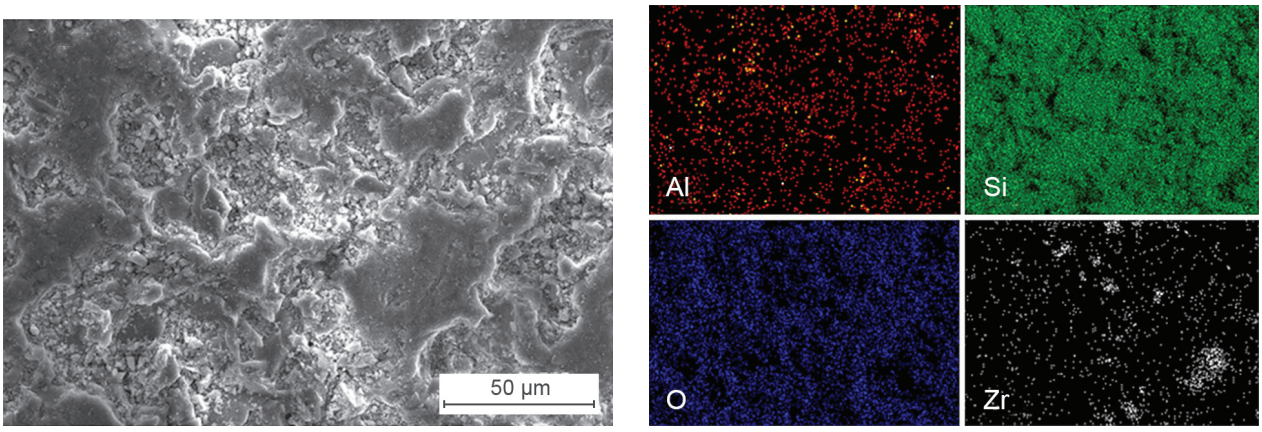

b) FNA-2

Figure 4. The EDS analysis results for the sintered ceramic specimens: a) FNA-0; b) FNA-2.

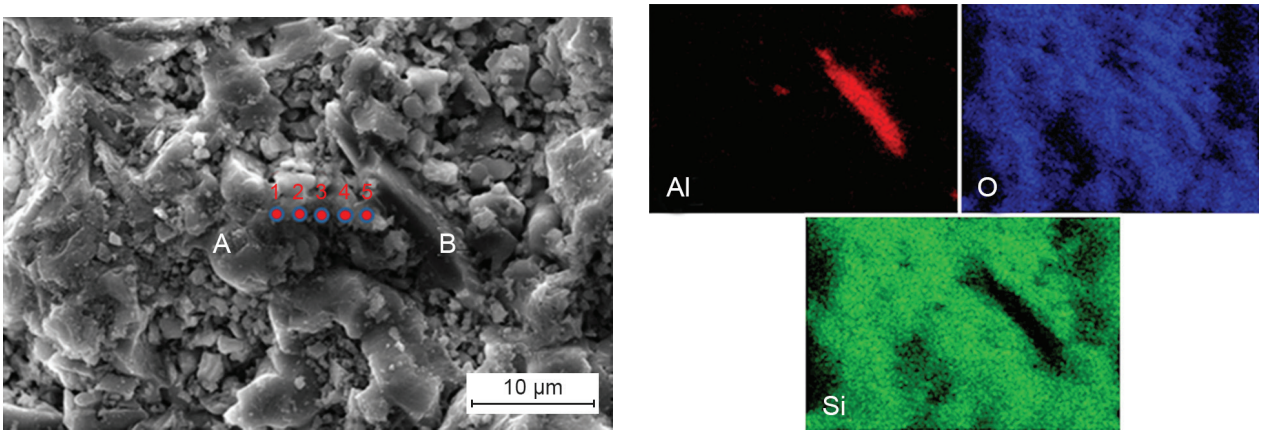

a) alumina microparticles

Figure 5. The EDS mapping result for a ceramic specimen with 4 wt. % added alumina sintered at 1300 °C: a) the added alumina microparticles. *(Continue on next page)*

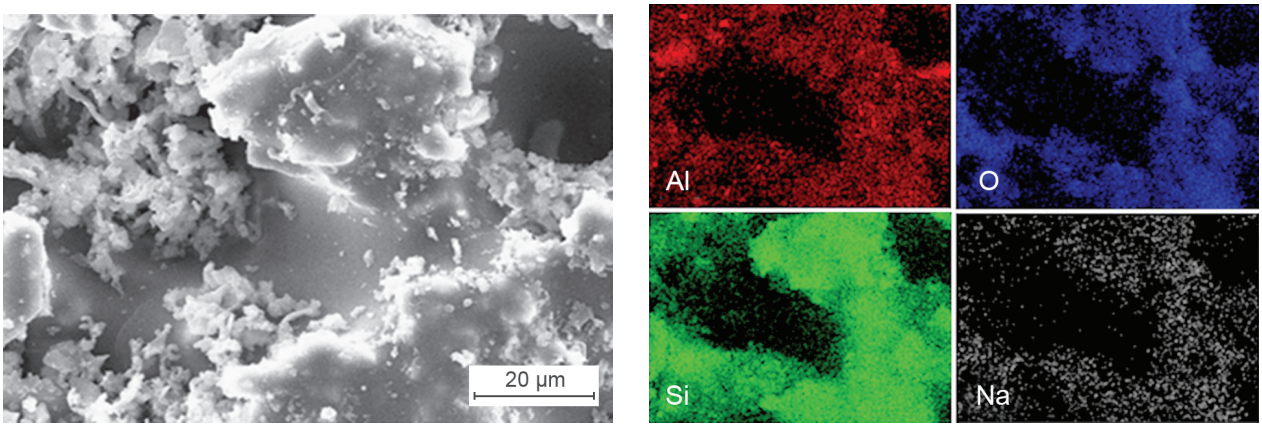

b) alumina nanoparticles

Figure 5. The EDS mapping result for a ceramic specimen with 4 wt. % added alumina sintered at 1300 °C: b) the added alumina nanoparticles.

weak sintering necks. Many small pores are observed around the fused silica particles. However, Figure 6d shows that the small pores between the particles are not observed in specimen FNA-2, but tiny and coarse particles are tightly adhered to each other by the liquid phase. The difference between specimens FNA-0 and FNA-2 can be observed more clearly in Figure 6e and f. For specimen FNA-0, a thin glass layer appears on the surface of a large fused silica particle. In addition, the microcrystalline groups are observed, which become the precursors for the cristobalite crystallisation and promote the crystallisation on the fused silica particles' surfaces. Nevertheless, in specimen FNA-2, the cristobalite grains on the fused silica particle surface begin to grow and aggregate, and those crystals are cemented by the liquid phase. This demonstrates that the addition of alumina nanoparticles is beneficial for the crystalliaation of cristobalite and for the formation of the liquid phase.

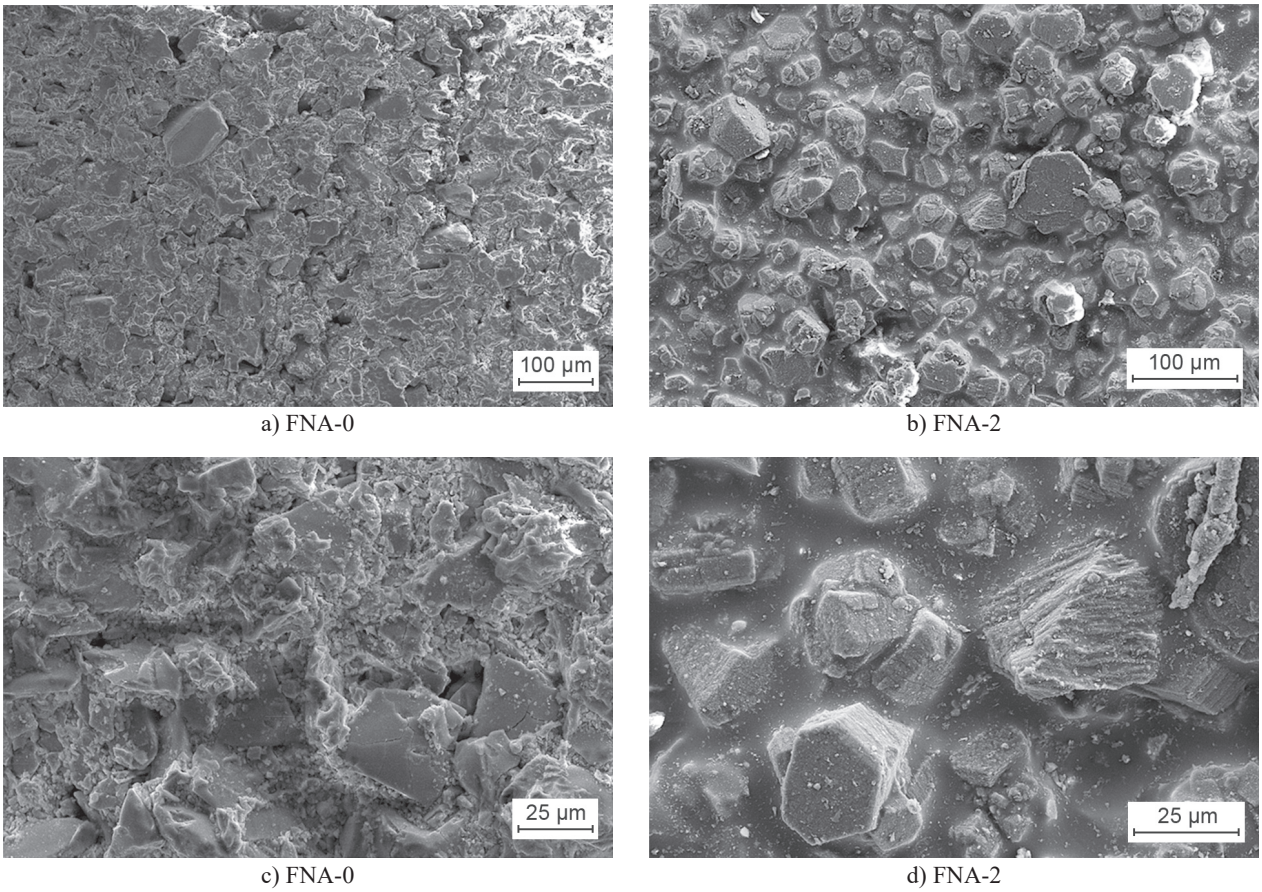

a) FNA-0 b) FNA-2

c) FNA-0 d) FNA-2

Figure 6. The microstructures of the ceramic specimens sintered at 1250 °C: a), c) FNA-0; b), d) FNA-2. *(Continue on next page)*

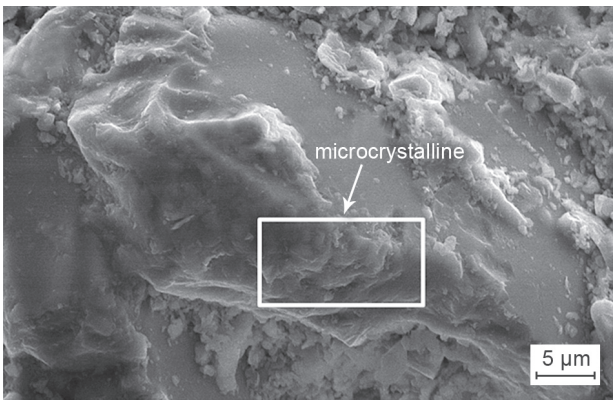

e) FNA-0

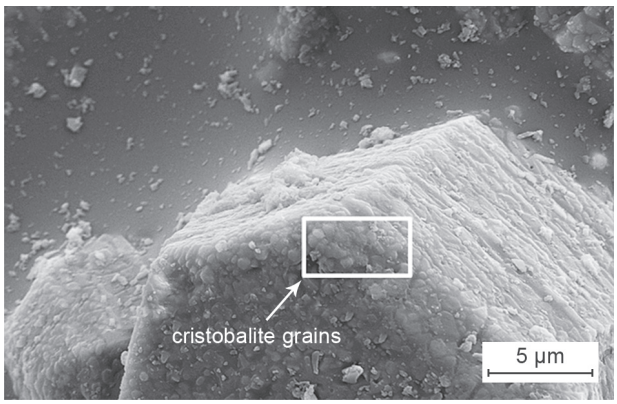

f) FNA-2

Figure 6. The microstructures of the ceramic specimens sintered at 1250 °C: e) FNA-0; f), d) FNA-2.

Figure 7 shows the EDS results for the liquid phase. Compared to the silica particle, in addition to a large amount of O and Si, other elements including Al, Na and K can be detected in the liquid phase (the alumina preparation process determines the amount of alkali and alkaline earth oxide impurities). Al, Na and K provide the liquid phase during the heat treatment, which flows into the pores between the particles. During the sintering, the liquid phase plays an important role in the densification [22]. When the sintering temperature exceeds the melting point of a specific component (e.g., alkaline feldspars and other alkali rich compounds) in the ceramic specimens or the glass transformation temperature of the amorphous fused silica phase in the raw material, the liquid phase can be formed. In addition, the viscosity of the liquid phase decreases at high temperatures,

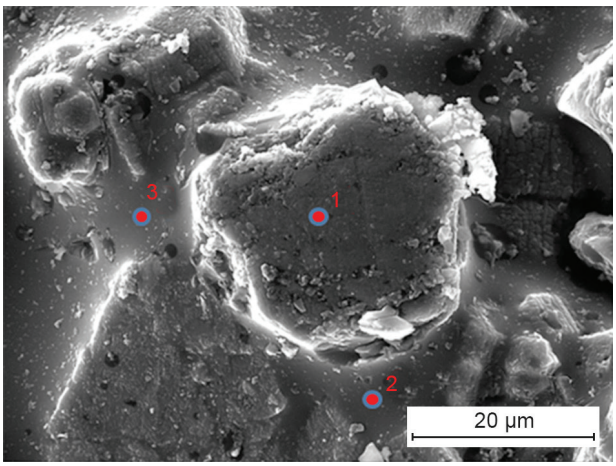

a)

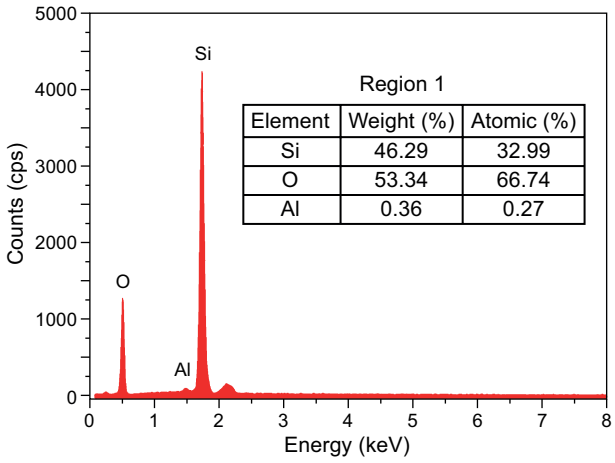

b)

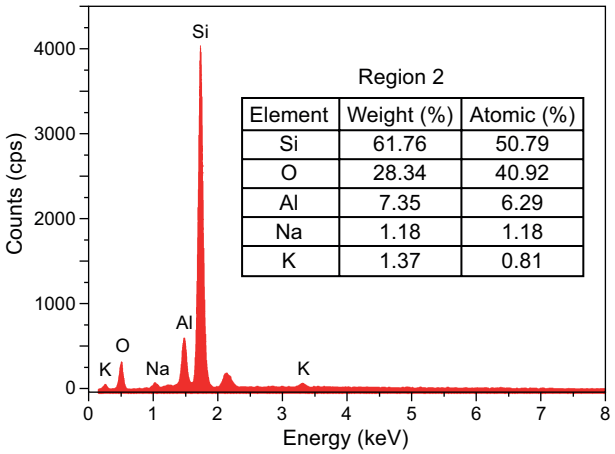

c)

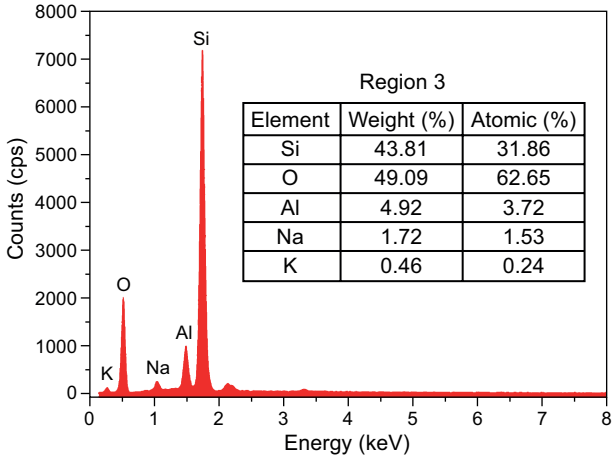

d)

Figure 7. The EDS results over several regions in specimen FNA-2.

allowing the liquid phase to flow and fill the pores under the action of surface tension, thus increasing the density of the ceramic specimens. As shown in Figure 8, the open porosities for the specimens sintered at 1250 °C are 32.71 % for FNA-0, 29.00 % for FNA-0.5, 28.73 % for FNA-1, 24.27 % for FNA-1.5, 20.12 % for FNA-2 and 19.33 % for FNA-2.5. When the sintering temperature increases to 1300 °C, the open porosities are 31.43 % for FNA-0, 27.92 % for FNA-0.5, 25.49 % for FNA-1, 21.33 % for FNA-1.5, 19.10 % for FNA-2 and 20.43 % for FNA-2.5. These results demonstrate that both the increase in the sintering temperature and the addition of the alumina nanoparticles are beneficial for increasing the densification and decreasing the open porosity of the silica-based ceramic specimens.

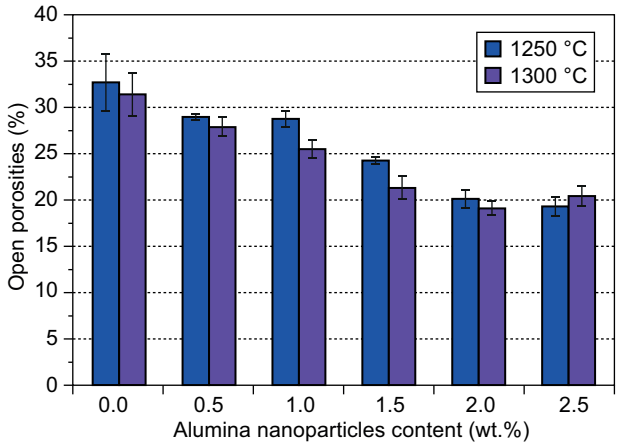

Figure 8. The open porosity of the sintered silica-based ceramic specimens.

Flexural strength

Figure 9 shows the flexural strength of the silica-based ceramic cores sintered at the different temperatures. There appears to be a quadratic relation of increasing the flexural strength with the increasing alumina nanoparticle concentration up to a certain level, and then either a plateau in the flexural strength or a reduction, regardless of the sintering temperature of 1250 °C or 1300 °C. This trend in the flexural strength is the same as that of specimens with the added alumina microparticles [10].

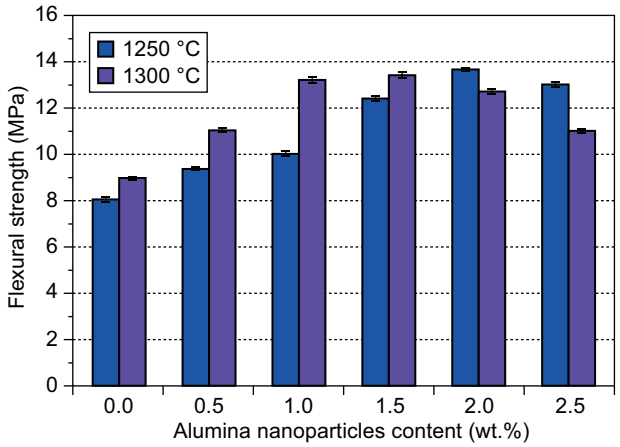

Figure 9. The flexural strength of the sintered silica-based ceramic specimens.

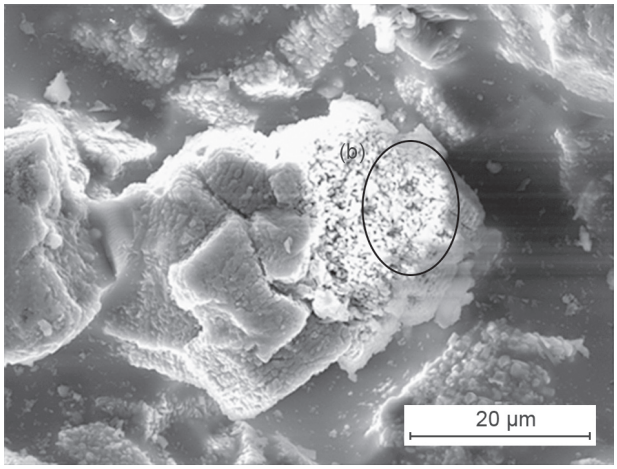

a)

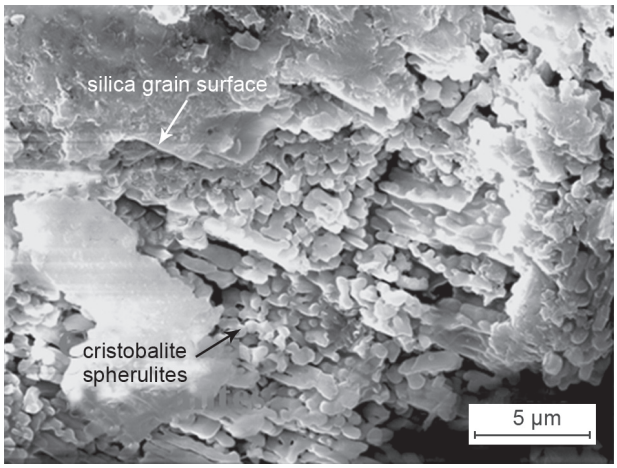

b)

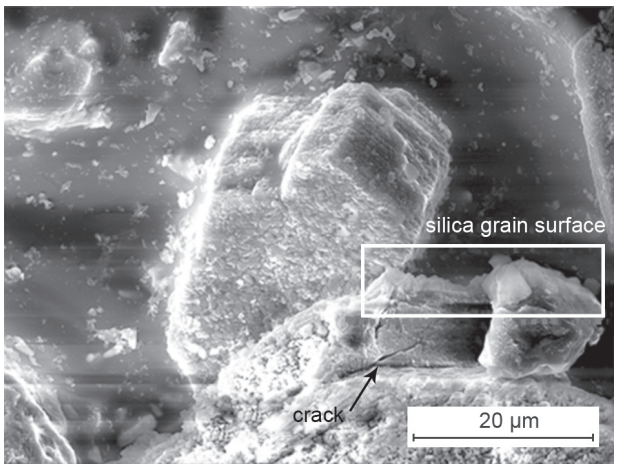

c)

Figure 10. The microstructures of ceramic specimen FNA-2.5 sintered at 1300 °C.

When the alumina nanoparticle concentration exceeds 2 wt. %, there is less strength enhancement due to the promotion of the cristobalite formation by the alumina. This is because the phase transformation from β-cristobalite to α-cristobalite can cause microcracks on the surface of the silica grains during the cooling from the sintering temperature [23, 24], decreasing the strength of the silica-based ceramic cores. As shown in Figure 10a, although there are no obvious cracks on the surface of the silica particles in specimen FNA-2.5 after sintering at 1300 °C, the cristobalite phase transformation during the cooling results in a loose silica particle structure. As shown in Figure 10b, the cristobalite spherulites inside the silica particles are connected together primarily in the form of point contacts. Additionally, the surfaces of the silica particles are filled with the liquid phase, resulting in a dense structure on the silica particle surface. Hence, the existence of a liquid phase is the reason why there are no obvious cracks on the surface of the silica particles. However, the volume shrinkage during cooling caused by a large amount of cristobalite grains inside the silica particles also leads to cracks, as shown in Figure 10c. The cracks penetrate into the silica particles, weakening the sintered silica.

Figure 11 shows the fractured surface of specimens FNA-0, FNA-0.5 and FNA-1, which were sintered at 1300 °C. The flexural strength enhancement of the silica-based ceramic specimens can be divided into two different stages: (1) in the specimens without the added alumina nanoparticles, the sintering necks between the particles are weak and easy to fracture. It can be proven that the propagation of the cracks in specimen FNA-0 occurs mainly through the sintering necks between the particles, and a large number of cracks appear on the silica particles' surfaces. Furthermore, the sintering necks are reinforced due to the liquid phase diffusion as the alumina nanoparticle concentration increases, which causes a mixed fracture path consisting of fractures along both the sintering necks and across the silica particles, as shown in specimen FNA-0.5. (2) when increasing the alumina nanoparticle concentration to 1.0 wt. %, the fracture path is mainly across the large particles. This is attributed to the further strengthening of the sintering necks. Hence, the strength of the silica particles plays the key role in enhancing the strength of the silica-based ceramic cores when the alumina nanoparticle content exceeds 1.0 wt. %. Though the presence of excessive cristobalite in the fused silica specimens leads to extensive cracking during the cooling, an appropriate amount of cristobalite transformed from the fused silica can provide stiffness in the ceramic specimens because the strength of the cristobalite is higher than that of fused silica. Furthermore, the surfaces of the silica particles are densified and strengthened by the liquid phase, decreasing the crack formation during the cooling. Consequently, more energy will be required to break the large particles. As shown in specimen FNA-1, the cleavage facets inside the large particles are clearly present on the fracture surface.

CONCLUSIONS

In this work, the effects of alumina nanoparticles on cristobalite crystallisation and the flexural strength of silica-based ceramic cores have been investigated. The main results are summarised as follows:

- The addition of alumina nanoparticles not only promotes the crystallisation of the fused silica, but also increases the formation of a liquid phase in the silica-based ceramic cores during the sintering. The increase in the liquid phase is mainly attributed to

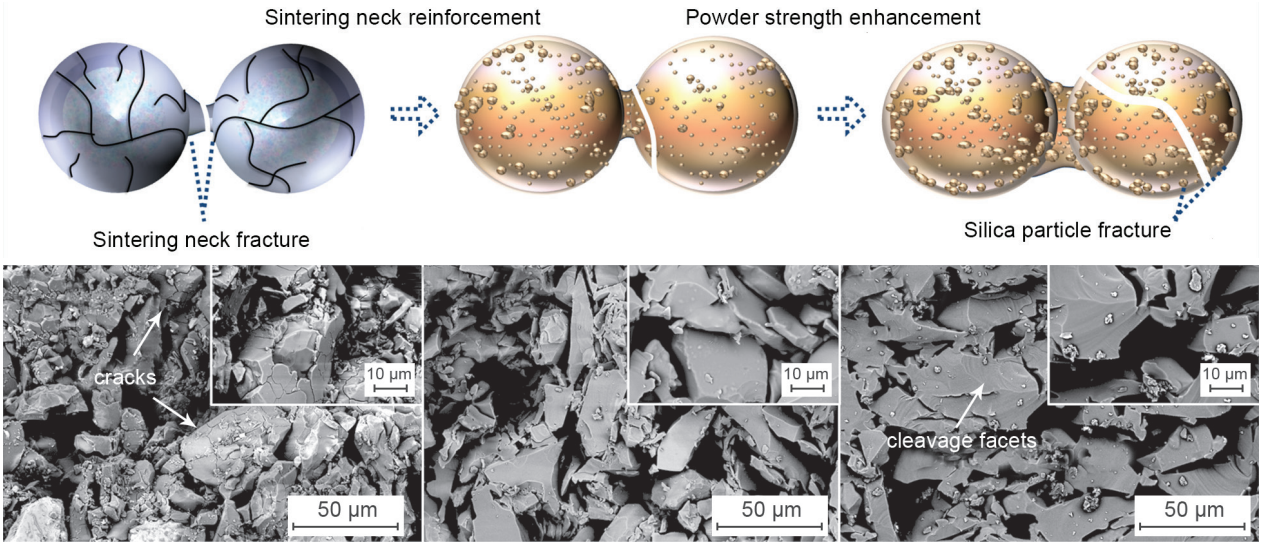

Figure 11. The schematic diagram of the sintering neck reinforcement and powder strength enhancement processes, together with the fractured surface of the silica-based ceramic specimens FNA-0, FNA-0.5 and FNA-1 sintered at 1300 °C.

the presence of Al, Na and K elements in the alumina nanoparticles, which diffuse into the pores as the liquid phase between the particles to improve densification. Compared to a specimen without added alumina nanoparticles, the open porosity of specimen FNA-2.5 decreases from 32.7 ± 3.01 % to 19.3 ± ± 1.04 % at 1250 °C and from 31.4 ± 2.32 % to 20.4 ± ± 1.08 %. at 1300 °C, respectively.

- The silica-based ceramic cores with a low alumina nanoparticle content (< 2.0 wt. %) were much more susceptible to strength enhancement than those with a high alumina nanoparticle content. This is because when the alumina nanoparticles content is above 2.0 wt. %, excessive cristobalite formation induces cracks in the sintered silica particles, decreasing the strength of the silica-based ceramic cores.
- The flexural strength of the silica-based ceramic cores increased from 8.98 ± 0.06 MPa to 13.42 ± 0.11 MPa when increasing the alumina nanoparticle content to 1.5 wt. % at 1300 °C. The increase in the strength of the silica-based ceramic cores at low alumina nanoparticle concentrations (< 1.0 wt. %) is attributed to the reinforced sintering necks between the particles. When the alumina nanoparticle content is above 1.0 wt. % (< 2.0 wt. %), the fracture path changes from along the sintering necks to across the particles, therefore, the strengthening of the silica grains plays a key role in increasing the flexural strength of the silica-based ceramic specimens.

Acknowledgments

This research did not receive any specific grant from funding agencies in the public, the commercial, or the non-profit sectors.

REFERENCES

1. Qin Y.X., Pan W. (2009): Effect of silica sol on the properties of alumina-based ceramic core composites, Materials Science and Engineering: A, 508, 71-75. doi: 10.1016/j.msea.2008.12.016
2. Gromada M., Świeca A., Kostecki M., Olszyna A., Cygan R. (2015): Ceramic cores for turbine blades via injection moulding, Journal of Materials Processing Technology, 220, 107-112. doi: 10.1016/j.jmatprotec.2015.01.010
3. Li K., Jiang W., Wang S., Xiao J., Lou L. (2018): Effect of specimen thickness on the creep deformation of a silica-based ceramic core material, Journal of Alloys and Compounds, 763, 781-790. doi: 10.1016/j.jallcom.2018.05.253
4. Pattnaik S., Karunakar D.B., Jha P.K. (2012): Developments in investment casting process – a review, Journal of Materials Processing Technology, 212, 2332-2348. doi: 10.1016/j.jmatprotec.2012.06.003
5. Kühn B., Schadrack R. (2009): Thermal expansion of synthetic fused silica as a function of OH content and fictive temperature, Journal of Non-crystalline Solids, 355, 323-326. doi: 10.1016/j.jnoncrysol.2008.11.005
6. Kruglov E.P., Kochetova G.K. (2007): Improvement of a technological process for ceramic core removal out of internal cavities of aircraft GTE turbine blade castings, Russian Aeronautics (IZ. VUZ), 50, 227-229. doi: 10.3103/s1068799807020201
7. Abo-mosallan H.A., Salama S.N., Salman S.M. (2016): Structure and characterization of some high chemically resistance silicate glasses, Ceramics Silikaty, 60, 263-272. doi: 10.13168/cs.2016.0039
8. Wan B., Zhang H., Ran C., Bai P., Zhang H. (2018): High-temperature wettability and interactions between NbSi-based alloys and Y_2O_3 ceramics, Ceramics International, 44, 32-39. doi: 10.1016/j.ceramint.2017.07.163
9. Kim E.H., Cho G.H., Yoo Y.S., Seo S.M., Jung Y.G. (2013): Development of a new process in high functioning ceramic core without shape deformation, Ceramics International, 39, 9041-9045. doi: 10.1016/j.ceramint.2013.04.107
10. Liang J.J., Lin Q.H., Zhang X., Jin T., Zhou Y.Z., Sun X.F., Choi B.G., Kim I.S., Do J.H., Jo C.Y. (2017): Effects of alumina on cristobalite crystallization and properties of silica-based ceramic cores, Journal of Materials Science & Technology, 33, 204-209. doi: 10.1016/j.jmst.2016.02.012
11. Breneman R.C., Halloran J.W. (2015): Effect of cristobalite on the strength of sintered fused silica above and below the cristobalite transformation, Journal of The American Ceramic Society, 98, 1611-1617. doi: 10.1111/jace.13505
12. Kim Y.H., Yeo J.G., Choi S.C. (2016): Shrinkage and flexural strength improvement of silica-based composites for ceramic cores by colloidal alumina infiltration, Ceramics International, 42, 8878-8883. doi: 10.1016/j.ceramint.2016.02.137
13. Bae C.-J., Kim D., Halloran J.W. (2019): Mechanical and kinetic studies on the refractory fused silica of integrally cored ceramic mold fabricated by additive manufacturing, Journal of the European Ceramic Society, 39, 618-623. doi: 10.1016/j.jeurceramsoc.2018.09.013
14. Kim Y.H., Yeo J.G., Lee J.S., Choi S.C. (2016): Influence of silicon carbide as a mineralizer on mechanical and thermal properties of silica-based ceramic cores, Ceramics International, 42, 14738-14742. doi: 10.1016/j.ceramint.2016.06.100
15. Kazemi A., Faghihi-Sani M.A., Nayyeri M.J., Mohammadi M., Hajfathalian M. (2014): Effect of zircon content on chemical and mechanical behavior of silica-based ceramic cores, Ceramics International, 40, 1093-1098. doi: 10.1016/j.ceramint.2013.06.108
16. Teng X.Y., Liu H.L., Huang C.Z. (2007): Effect of Al_2O_3 particle size on the mechanical properties of alumina-based ceramics, Materials Science and Engineering: A, 452, 545-551. doi: 10.1016/j.msea.2006.10.073
17. Ji Y., Yeomans J.A. (2002), Processing and mechanical properties of Al_2O_3–5 vol.% Cr nanocomposites, Journal of the European Ceramic Society, 22, 1927-1936. doi: 10.1016/s0955-2219(01)00528-3
18. Hassan A.M., Awaad M., Bendioli F., Naga S.M. (2014): Densification behavior and mechanical properties of niobium oxide doped alumina ceramics, Journal of Materials Science & Technology, 5, 51-56. doi: 10.4416/JCST2013-00045

19. Liu J., Zhu T., Xie Z.P., Wu W. (2017): New route to improve the flexural strength of silicon nitride ceramics by introducing tungsten carbide nanoparticles, International journal of Applied Ceramic Technology, 14, 860-865. doi: 10.1111/ijac.12732
20. Snyder R.L. (1992): The use of reference intensity ratios in X-ray quantitative analysis, Powder Diffraction, 7, 186-193. doi: 10.1017/s0885715600018686
21. Kazemi A., Faghihi-Sani M.A., Alizadeh H.R. (2013): Investigation on cristobalite crystallization in silica-based ceramic cores for investment casting, Journal of the European Ceramic Society, 33, 3397-3402. doi: 10.1016/j.jeurceramsoc.2013.06.025
22. Shao J.Q., Li M., Chang K.K., Huang Y., Ren D.L., Wang J., Zhou X.B., He L., Huang F., Du S.Y., Sha J.J., Huang Z.R., Huang Q. (2018): Fabrication and characterization of SPS sintered SiC-based ceramic from $Y_3Si_2C_2$-coated SiC powders, Journal of the European Ceramic Society, 38, 4833-4841. doi: 10.1016/j.jeurceramsoc.2018.07.054
23. Wisniewski W., Berndt S., Müller M., Rüssel C. (2013): Stress induced texture formation in surface crystallized SiO_2 glass, CrystEngComm, 15, 2392-2400. doi: 10.1039/c3ce26843h
24. Pascova R., AvdeeG. v, Gutzow I., Penkov I., Ludwing F.-P., Schmelzer J.W.P. (2012): Refractory alkali-free cristobalite glass-ceramics: activated reaction sinter-crystallization synthesis and properties, International Journal of Applied Glass Science, 3, 75-87. doi: 10.1111/ j.2041-1294.2011.00072.x